

Crystal structure of the (1*R*,2*S*,5*R*) diastereomer of acoltremon, C₁₈H₂₇NO₂, from synchrotron powder diffraction data and density functional theory calculations

Jacob K. Salazar,^a James A. Kaduk,^{b,c,*} Anja Dosen^d and Thomas N. Blanton^d

Received 21 April 2026

Accepted 22 June 2026

Edited by W. T. A. Harrison, University of Aberdeen, United Kingdom

Keywords: powder diffraction; acoltremon; Tryptyr; Rietveld refinement; density functional theory.

CCDC references: 2564140; 2564139; 2564138

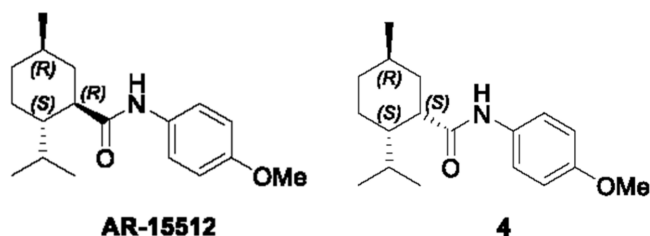
Supporting information: this article has supporting information at journals.iucr.org/e

^aNorth Central College, Department of Chemistry, 131 S. Loomis St., Naperville IL 60540, USA, ^bNorth Central College, Department of Physics, 131 S. Loomis St., Naperville IL 60540, USA, ^cIllinois Institute of Technology, Department of Chemistry, 3101 S. Dearborn St., Chicago IL 60616, USA, and ^dICDD, 12 Campus Blvd., Newtown Square, PA 19073-3273, USA. *Correspondence e-mail: kaduk@polycrystallography.com

The crystal structure of the (1*R*,2*S*,5*R*) diastereomer of acoltremon [systematic name: (1*R*,2*S*,5*R*)-2-isopropyl-*N*-(4-methoxyphenyl)-5-methylcyclohexane-1-carboxamide], C₁₈H₂₇NO₂, has been solved and refined using synchrotron X-ray powder diffraction data, and optimized using density functional theory techniques. Acoltremon crystallizes in space group *P*2₁2₁2₁ and the crystal structure consists of corrugated layers lying parallel to the *bc* plane. N—H···O hydrogen bonds link the molecules into chains propagating along the *a*-axis direction, with graph-set descriptor *C*₁¹(4).

1. Chemical context

Acoltremon, C₁₈H₂₇NO₂ (sold under the brand name Tryptyr in the United States, and also known as AR-15512) is used to treat dry-eye syndrome. It is administered as a preservative free dilute solution in eye drops for the purpose of increasing basal tears production. The systematic name (CAS Registry Number 68489-09-8) is (1*R*,2*S*,5*R*)-*N*-(4-methoxyphenyl)-5-methyl-2-propan-2-ylcyclohexane-1-carboxamide.

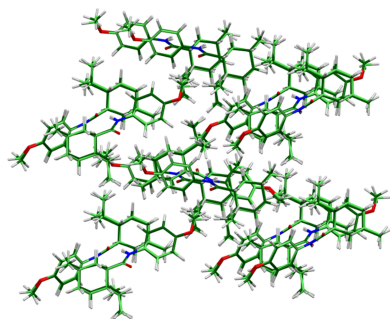


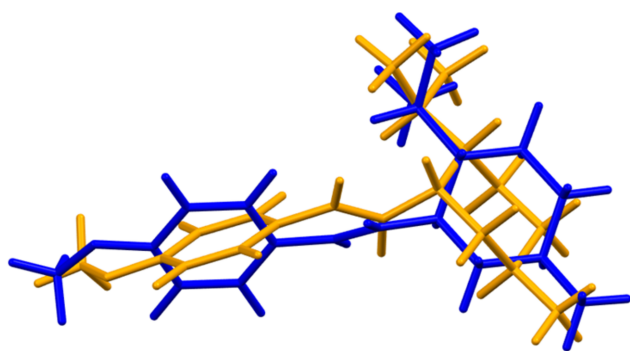
A crystal structure of acoltremon at 100 K has been reported (Rodríguez-Arévalo *et al.*, 2021), but it is of the (1*S*,2*S*,5*R*) diastereomer, **4**, and not the active pharmaceutical. We are unaware of any published powder diffraction data on the (1*R*,2*S*,5*R*) diastereomer.

This work was carried out as part of a project (Kaduk *et al.*, 2014) to determine the crystal structures of large-volume commercial pharmaceuticals, and includes depositing high-quality powder diffraction data for them in the Powder Diffraction File (Kabekkodu *et al.*, 2024).

2. Structural commentary

The dispersion-corrected *VASP* calculations indicate that the structure of the (1*R*,2*S*,5*R*) diastereomer determined here is





Blue = ours; orange = 100K; rms delta = 1.206

Figure 1

Comparison of the (1*R*,2*S*,5*R*) diastereomer characterized in this study (blue) to the (1*S*,2*S*,5*R*) diastereomer characterized by Rodríguez-Arévalo *et al.* (2021; orange). The root-mean-square Cartesian displacement is 1.206 Å.

23.3 kcal mol⁻¹ lower in energy than that of the (1*S*,2*S*,5*R*) diastereomer determined by Rodríguez-Arévalo *et al.* (2021) (see Table 5 in the supporting information). As expected, the molecules are quite different (Fig. 1), with a root-mean-square Cartesian displacement of 1.206 Å.

The root-mean-square difference of the non-H atoms in the Rietveld-refined and *VASP*-optimized structures of acoltremon, calculated using the *Mercury* (Macrae *et al.*, 2020) CSD-Materials/Search/Crystal Packing Similarity tool is 0.133 Å (Fig. 2); the structures are essentially identical. The root-mean-square Cartesian displacement of the non-H atoms

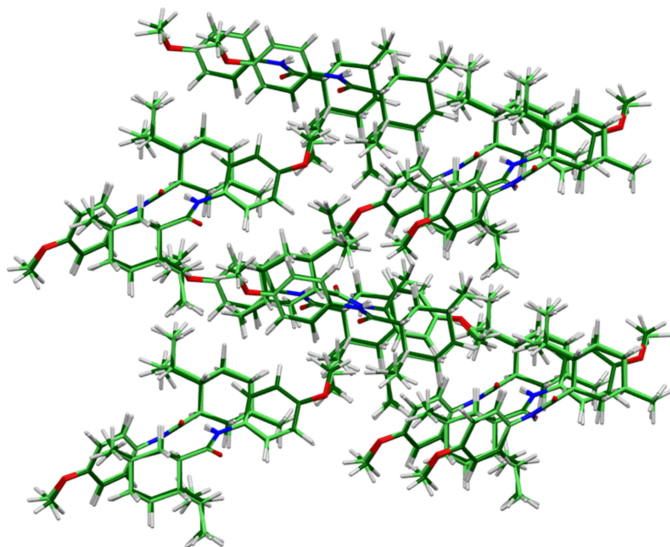


Figure 2

Comparison of the Rietveld-refined (colored by atom type) and *VASP*-optimized (pale green) structures of acoltremon, calculated using the *Mercury* CSD-Materials/Search/Crystal Packing Similarity tool. The root-mean-square Cartesian displacement is 0.133 Å.

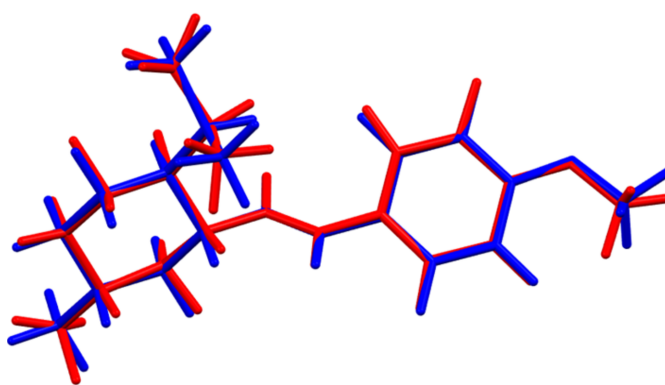


Figure 3

Comparison of the refined structure of acoltremon (red) to the *VASP*-optimized structure (blue). The comparison was generated using the *Mercury* Calculate/Molecule Overlay tool; the root-mean-square Cartesian displacement is 0.108 Å.

in the refined and optimized structures, calculated using the *Mercury* Calculate/molecule overlay tool, is 0.108 Å (Fig. 3). The agreements are within the normal range for correct structures (van de Streek & Neumann, 2014). The asymmetric unit is illustrated in Fig. 4. The remaining discussion will emphasize the *VASP*-optimized structure.

All the bond distances, bond angles, and torsion angles fall within the normal ranges indicated by a *Mercury* Mogul geometry check (Macrae *et al.*, 2020). Quantum chemical geometry optimization of the isolated acoltremon molecule (DFT/B3LYP/6-31G*/water) using *Spartan '24* (Wavefunction, 2025) indicated that the observed conformation lies 2.7 kcal mol⁻¹ above a local minimum, which has a similar overall conformation (r.m.s. displacement = 0.338 Å); the difference is mainly in the orientation of the phenyl ring. Similarly, the observed conformation of the (1*S*,2*S*,5*R*) diastereomer lies 3.4 kcal mol⁻¹ higher in energy than a local minimum, which differs more (r.m.s. displacement = 0.653 Å), mainly in the orientations of the isopropyl, methyl, and phenyl groups. These single-molecule calculations indicate that the diaster-

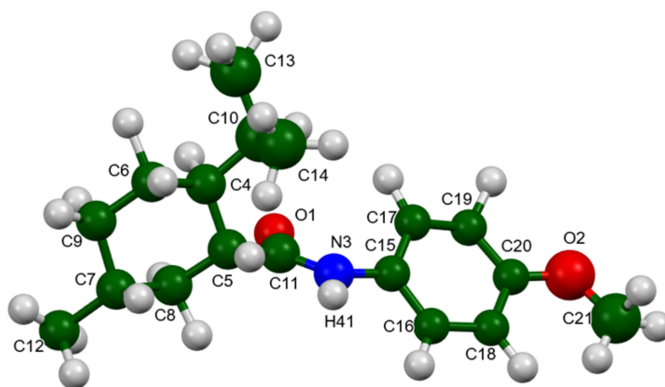


Figure 4

The asymmetric unit of acoltremon, with the atom numbering. The atoms are represented by 50% probability spheroids.

Table 1
Hydrogen-bond geometry (Å, °) for VASP-optimized acoltremon.

$D-H\cdots A$	$D-H$	$H\cdots A$	$D\cdots A$	$D-H\cdots A$	Mulliken overlap	H-bond energy
N3–H41 \cdots O1 ⁱ	1.04	1.80	2.836	175	0.064	5.8
C5–H23 \cdots O1 ⁱ	1.10	2.47	3.428	145	0.014	–
C13–H35 \cdots O2	1.10	2.61	3.594	148	0.010	–
C10–H31 \cdots C11 ⁱⁱ	1.11	2.50	2.991	106	0.012	–

Symmetry codes: (i) $-x - 1, y + \frac{1}{2}, -z + \frac{3}{2}$; (ii) $x + \frac{5}{2}, -y - \frac{1}{2}, -z + 1$.

Table 2
Hydrogen-bond geometry (Å, °) for VASP-optimized (1*S*,2*S*,5*R*) diastereomer.

$D-H\cdots A$	$D-H$	$H\cdots A$	$D\cdots A$	$D-H\cdots A$	Mulliken overlap	H-bond energy
N1–H1 <i>N</i> \cdots O1 ⁱ	1.03	1.89	2.922	176	0.048	5.1
C18–H18 <i>B</i> \cdots O1 ⁱⁱ	1.10	2.30	3.383	169	0.022	–
C10–H10 \cdots O1 ⁱⁱⁱ	1.10	2.48	3.466	149	0.016	–
C9–H9 <i>B</i> \cdots O2	1.10	2.61	3.526	140	0.011	–
C3–H00 <i>F</i> \cdots C11	1.11	2.55	2.963	101	0.011	–

Symmetry codes: (i) $-x + 1, y + \frac{3}{2}, -z + \frac{3}{2}$; (ii) $x + \frac{5}{2}, -y - \frac{1}{2}, -z + 1$; (iii) $-x - 1, y + \frac{3}{2}, -z + \frac{3}{2}$.

omer of this study is 2.4 kcal mol^{−1} more stable than the other one.

3. Supramolecular features

A view down the *a* axis of the crystal structure (Fig. 5) shows the molecules clearly, but a view down the *c* axis (Fig. 6) makes

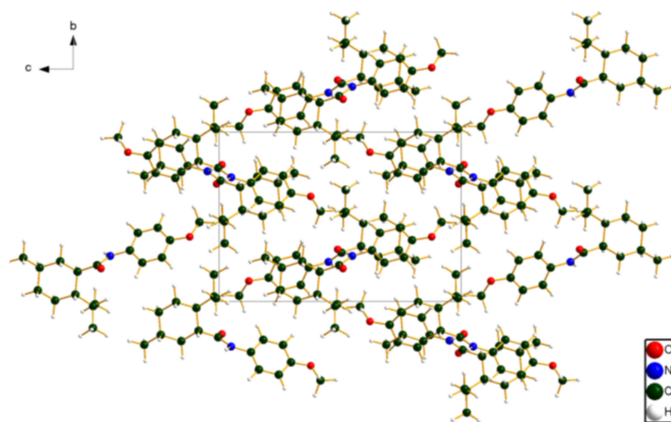


Figure 5
The unit-cell packing of acoltremon, viewed down the *a*-axis direction.

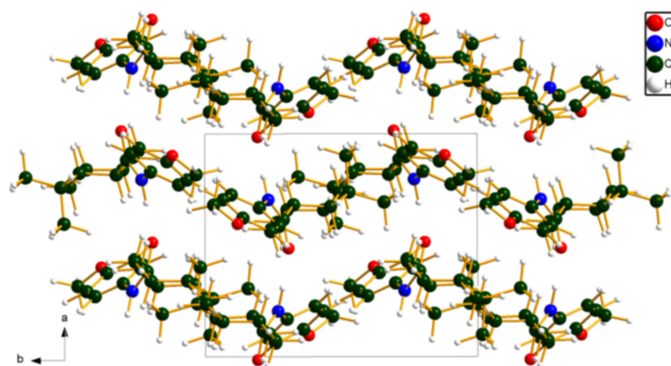


Figure 6
The unit-cell packing of acoltremon, viewed down the *c*-axis direction.

it clear that the structure consists of corrugated layers lying parallel to the *bc* plane. The *Mercury* aromatics analyser indicates only extremely weak phenyl–phenyl interactions, with distances ≥ 8.56 Å. The mean Miller plane of the molecule is approximately (721).

Analysis of the contributions to the total crystal energy of the structure using the forcite module of *Materials Studio* (Dassault Systèmes, 2025) indicated that bond, angle, and torsion distortion terms contribute about equally to the intramolecular energy. The intermolecular energy is dominated by van der Waals attractions, which in this force field based analysis include hydrogen bonds. The hydrogen bonds are better discussed using the results of the DFT calculation.

The hydrogen bonds are summarized in Tables 1 and 2. In both the (1*R*,2*S*,5*R*) diastereomer studied here and the (1*S*,2*S*,5*R*) diastereomer of Rodríguez-Arévalo *et al.* (2021), the amino and carbonyl groups link the molecules into chains (Fig. 7) propagating along the *a*-axis direction, with graph-set descriptor (Etter, 1990; Bernstein *et al.*, 1995; Motherwell *et al.*, 2000) $C_1^1(4)$. These chains link the corrugated layers. However, the patterns of C–H \cdots O and C–H \cdots C hydrogen bonds are almost completely different between the two diastereomers.

The volume enclosed by the Hirshfeld surface of acoltremon (Fig. 9; Spackman *et al.*, 2021) is 424.36 Å³, 98.31% of 1/4 of the unit-cell volume. The packing density is thus typical.

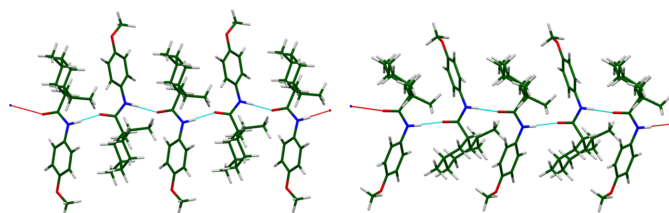


Figure 7
The hydrogen bond chains in the (1*R*,2*S*,5*R*) diastereomer characterized in this study (left) and the (1*S*,2*S*,5*R*) diastereomer (right) characterized by Rodríguez-Arévalo *et al.* (2021). In each case the crystallographic *a* axis is horizontal.

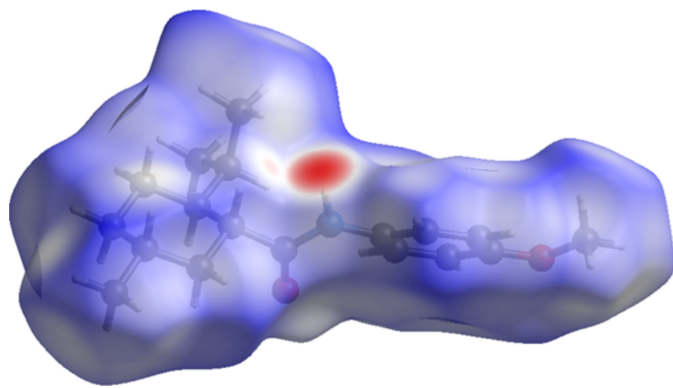


Figure 8
The Hirshfeld surface of acoltremon. Intermolecular contacts longer than the sums of the van der Waals radii are colored blue, and contacts shorter than the sums of the radii are colored red. Contacts equal to the sums of radii are white.

The only significant close contacts (red in Fig. 8) involve the hydrogen bonds. The volume/non-hydrogen atom is larger than normal, at 20.5 \AA^3 .

The Bravais–Friedel–Donnay–Harker (Bravais, 1866; Friedel, 1907; Donnay & Harker, 1937) algorithm suggests that we might expect isotropic morphology for acoltremon. A second-order spherical harmonic model for preferred orientation was included. The texture index was 1.034, indicating that the preferred orientation was slight in this rotated capillary specimen.

4. Database survey

A reduced cell search in the Cambridge Structural Database (CSD 2026.1.0; Groom *et al.*, 2016), combined with the chemistry C, H, N, and O only, yielded 22 hits, but no structures for acoltremon or its derivatives.

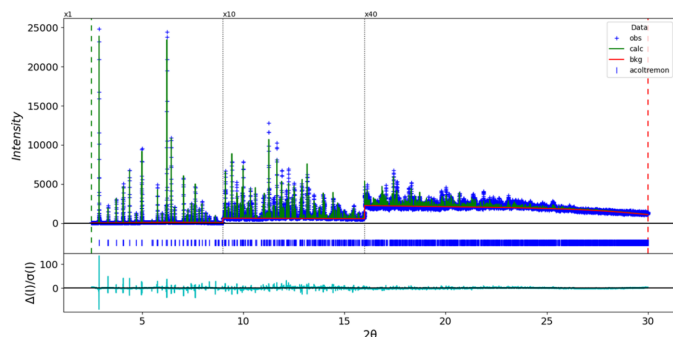


Figure 9
The Rietveld plot for acoltremon. The blue crosses represent the observed data points, and the green line is the calculated pattern. The cyan curve is the normalized error plot, and the red line is the background curve. The blue tick marks indicate the peak positions. The vertical scale has been multiplied by a factor of $10\times$ for $2\theta > 9.0^\circ$ and by a factor of $40\times$ for $2\theta > 16.0^\circ$.

Table 3
Experimental details.

		acoltremon_2
Crystal data		
Chemical formula		$\text{C}_{18}\text{H}_{27}\text{NO}_2$
M_r		289.42
Crystal system, space group		Orthorhombic, $P2_12_12_1$
Temperature (K)		295
a, b, c (Å)		9.320220 (15), 11.39111 (3), 16.26284 (4)
V (Å ³)		1726.59 (1)
Z		4
Radiation type		Synchrotron, $\lambda = 0.46873 \text{ \AA}$
μ (mm ⁻¹)		0.005
Specimen shape, size (mm)		Cylinder, 2.0×1.5
Data collection		
Diffractometer		11-BM, APS
Specimen mounting		Kapton capillary
Data collection mode		Transmission
Scan method		Step
2θ values (°)		$2\theta_{\min} = 0.510$, $2\theta_{\max} = 49.995$, $2\theta_{\text{step}} = 0.001$
Refinement		
R factors and goodness of fit		$R_p = 0.113$, $R_{wp} = 0.133$, $R_{\text{exp}} = 0.038$, $R(F^2) = 0.10052$, $\chi^2 = 12.888$
No. of parameters		83
No. of restraints		53
$(\Delta/\sigma)_{\max}$		1.712

Computer programs: *GSAS-II* (Toby & Von Dreele, 2013) and *DIAMOND* (Brandenburg & Putz, 2025).

5. Synthesis and crystallization

Acoltremon is a commercial reagent and was purchased from TargetMol (Batch #141432) and used as-received.

6. Refinement

Crystal data, data collection and structure refinement details are summarized in Table 3. The white powder was packed into a 1.5 mm diameter Kapton capillary, and rotated during the measurement at $\sim 50 \text{ Hz}$. The powder pattern was measured at 295 K at beam line 11-BM (Lee *et al.*, 2008; Wang *et al.*, 2008; Antao *et al.*, 2008) of the Advanced Photon Source at Argonne National Laboratory using a wavelength of 0.4687342 \AA from $0.5\text{--}50^\circ 2\theta$ with a step size of 0.001° and a counting time of $0.1 \text{ sec step}^{-1}$. The high-resolution powder diffraction data were collected using twelve silicon crystal analyzers that allow for high angular resolution, high precision, and accurate peak positions. A mixture of silicon (NIST SRM 640c) and alumina (NIST SRM 676a) standards (ratio $\text{Al}_2\text{O}_3:\text{Si} = 2:1$ by weight) was used to calibrate the instrument and refine the monochromatic wavelength used in the experiment.

The pattern was indexed on a primitive orthorhombic unit cell with $a = 9.32059$, $b = 11.39187$, $c = 16.25977 \text{ \AA}$, $V = 1727.5 \text{ \AA}^3$, and $Z = 4$ using *N-TREOR* as incorporated into *EXPO2014* (Altomare *et al.*, 2013). The suggested space group was $P2_12_12_1$, which was confirmed by successful solution and refinement of the structure.

The *a*, *b*, and *c* lattice parameters at 298 K were 2.0% larger, 9.7% larger, and 7.0% smaller than those reported at 100 K. Refinement was started using the fractional coordinates of Rodriguez-Arévalo *et al.* (2021), before we realized that they were for a different diastereomer. The refinement changed the chiralities to result in the enantiomer of the correct diastereomer.

To make a cleaner narrative, the molecular structure of (1*R*,2*S*,5*R*)-acoltremone was downloaded from PubChem (Kim *et al.*, 2023) as Conformer3D_COMPOUND_CID_11266244.sdf. It was converted to a *.mol2 file using Mercury (Macrae *et al.*, 2020). The structure was solved using Monte Carlo simulated annealing techniques as implemented in EXPO2014 (Altomare *et al.*, 2013).

Rietveld refinement was carried out using GSAS-II (Toby & Von Dreele, 2013). Only the 2.5–30.0° portion of the pattern was included in the refinements ($d_{min} = 0.905 \text{ \AA}$). The μR value was fixed at 0.00, calculated using the 11-BM website (<https://11bm.xray.aps.anl.gov/absorb/>). All non-H bond distances and angles were subjected to restraints, based on a Mercury Mogul geometry check (Sykes *et al.*, 2011; Bruno *et al.*, 2004). The Mogul average and standard deviation for each quantity were used as the restraint parameters. The aromatic ring was restrained to be planar. The restraints contributed 4.0% to the overall χ^2 . The hydrogen atoms were included in calculated positions, which were recalculated during the refinement using Materials Studio (Dassault Systèmes, 2024). The $U_{iso}(H)$ values were grouped by chemical similarity. The peak profiles were described using an isotropic microstrain model, with the strain fixed at 10 ppm. The background was modeled using a six-term shifted Chebyshev polynomial, with a peak at 6.17° to model the scattering from the Kapton capillary and any amorphous component of the sample.

The final refinement of 83 variables using 27,501 observations and 53 restraints yielded the residuals $R_{wp} = 0.1352$ and GOF = 3.59. The largest peak (0.13 Å from C15) and hole (1.19 Å from C10) in the difference Fourier map are 1.07 (16) and $-0.67 (16) e \text{ \AA}^{-3}$, respectively. The final Rietveld plot is shown in Fig. 9. The largest features in the normalized error plot are in the positions and shapes of some of the strong low-angle peaks, and may indicate a change in the specimen during the measurement.

The crystal structures of both diastereomers were optimized (fixed experimental unit cells) with density functional theory techniques using VASP (Kresse & Furthmüller, 1996) through the MedeA graphical interface (Materials Design, 2024). The calculations were carried out on 32 cores of a 144-core (768 Gb memory) HPE Superdome Flex 280 Linux server at North Central College. The calculation used the GGA-PBE functional, a plane wave cutoff energy of 400.0 eV, and a *k*-point spacing of 0.5 \AA^{-1} leading to a $2 \times 2 \times 1$ mesh. To permit comparison of the energies and lattice parameters of the two diastereomers, dispersion-corrected DFT calculations were also carried out using VASP, incorporating the DFT-D3 approach of Grimme and allowing the lattice parameters to optimize. Single-point density functional theory calculations (fixed experimental cell) and population analysis were carried

out using CRYSTAL23 (Erba *et al.*, 2023). (fixed experimental cell) and population analysis were carried out using CRYSTAL17 (Dovesi *et al.*, 2018). The basis sets for the H, C, N and O atoms in the calculation were those of Gatti *et al.* (1994). The calculations were run on a 3.5 GHz PC using 8 *k*-points and the B3LYP functional.

Acknowledgements

Use of the Advanced Photon Source at Argonne National Laboratory was supported by the U. S. Department of Energy, Office of Science, Office of Basic Energy Sciences, under Contract No. DE-AC02-06CH11357. We thank Saul Lapidus for his assistance in the data collection. We also thank the ICDD team – Megan Rost, Steve Trimble, and Dave Bohnenberger – for their contribution to research, sample preparation, and in-house XRD data collection and verification.

Funding information

Funding for this research was provided by: International Centre for Diffraction Data (grant No. 09-03).

References

- Altomare, A., Cuocci, C., Giacovazzo, C., Moliterni, A., Rizzi, R., Corriero, N. & Falcicchio, A. (2013). *J. Appl. Cryst.* **46**, 1231–1235.
- Antao, S. M., Hassan, I., Wang, J., Lee, P. L. & Toby, B. H. (2008). *Can. Mineral.* **46**, 1501–1509.
- Bernstein, J., Davis, R. E., Shimon, L. & Chang, N. L. (1995). *Angew. Chem. Int. Ed. Engl.* **34**, 1555–1573.
- Brandenburg, K. & Putz, H. (2025). *DIAMOND V 5.1.1*. Crystal Impact, Bonn, Germany.
- Bravais, A. (1866). *Etudes Cristallographiques*. Paris: Gauthier Villars.
- Bruno, I. J., Cole, J. C., Kessler, M., Luo, J., Motherwell, W. D. S., Purkis, L. H., Smith, B. R., Taylor, R., Cooper, R. I., Harris, S. E. & Orpen, A. G. (2004). *J. Chem. Inf. Comput. Sci.* **44**, 2133–2144.
- Dassault Systèmes (2025). *BIOVIA Materials Studio 2025*. San Diego, CA: BIOVIA.
- Donnay, J. D. H. & Harker, D. (1937). *Am. Mineral.* **22**, 446–467.
- Dovesi, R., Erba, A., Orlando, R., Zicovich-Wilson, C. M., Civalleri, B., Maschio, L., Rérat, M., Casassa, S., Baima, J., Salustro, S. & Kirtman, B. (2018). *WIREs Comput. Mol. Sci.* **8**, e1360.
- Erba, A., Desmarais, J. K., Casassa, S., Civalleri, B., Donà, L., Bush, I. J., Searle, B., Maschio, L., Edith-Daga, L., Cossard, A., Ribaldone, C., Ascricchi, E., Marana, N. L., Flament, J.-P. & Kirtman, B. (2023). *J. Chem. Theory Comput.* **19**, 6891–6932.
- Etter, M. C. (1990). *Acc. Chem. Res.* **23**, 120–126.
- Friedel, G. (1907). *Bull. Soc. Fr. Min.* **30**, 326–455.
- Gatti, C., Saunders, V. R. & Roetti, C. (1994). *J. Chem. Phys.* **101**, 10686–10696.
- Groom, C. R., Bruno, I. J., Lightfoot, M. P. & Ward, S. C. (2016). *Acta Cryst.* **B72**, 171–179.
- Kabekkodu, S., Dosen, A. & Blanton, T. N. (2024). *Powder Diffr.* **39**, 47–59.
- Kaduk, J. A., Crowder, C. E., Zhong, K., Fawcett, T. G. & Suchomel, M. R. (2014). *Powder Diffr.* **29**, 269–273.
- Kim, S., Chen, J., Cheng, T., Gindulyte, A., He, J., He, S., Li, Q., Shoemaker, B. A., Thiessen, P. A., Yu, B., Zaslavsky, L., Zhang, J. & Bolton, E. E. (2023). *Nucleic Acids Res.* **51**, D1373–D1380.
- Kresse, G. & Furthmüller, J. (1996). *Comput. Mater. Sci.* **6**, 15–50.

- Lee, P. L., Shu, D., Ramanathan, M., Preissner, C., Wang, J., Beno, M. A., Von Dreele, R. B., Ribaud, L., Kurtz, C., Antao, S. M., Jiao, X. & Toby, B. H. (2008). *J. Synchrotron Rad.* **15**, 427–432.
- Macrae, C. F., Sovago, I., Cottrell, S. J., Galek, P. T. A., McCabe, P., Pidcock, E., Platings, M., Shields, G. P., Stevens, J. S., Towler, M. & Wood, P. A. (2020). *J. Appl. Cryst.* **53**, 226–235.
- Materials Design. (2024). *MedeA 3.7.2*. Materials Design Inc., San Diego, USA.
- Motherwell, W. D. S., Shields, G. P. & Allen, F. H. (2000). *Acta Cryst.* **B56**, 857–871.
- Rodríguez-Arévalo, S., Pujol, E., Abás, S., Galdeano, C., Escolano, C. & Vázquez, S. (2021). *Molecules* **26**, 906.
- Spackman, P. R., Turner, M. J., McKinnon, J. J., Wolff, S. K., Grimwood, D. J., Jayatilaka, D. & Spackman, M. A. (2021). *J. Appl. Cryst.* **54**, 1006–1011.
- Streek, J. van de & Neumann, M. A. (2014). *Acta Cryst.* **B70**, 1020–1032.
- Sykes, R. A., McCabe, P., Allen, F. H., Battle, G. M., Bruno, I. J. & Wood, P. A. (2011). *J. Appl. Cryst.* **44**, 882–886.
- Toby, B. H. & Von Dreele, R. B. (2013). *J. Appl. Cryst.* **46**, 544–549.
- Wang, J., Toby, B. H., Lee, P. L., Ribaud, L., Antao, S. M., Kurtz, C., Ramanathan, M., Von Dreele, R. B. & Beno, M. A. (2008). *Rev. Sci. Instrum.* **79**, 085105.
- Wavefunction (2025). *Spartan '24. V. 1.3.1*. Wavefunction Inc., Irvine, USA.

supporting information

Acta Cryst. (2026). E82, 877-882 [https://doi.org/10.1107/S2056989026006572]

Crystal structure of the (1*R*,2*S*,5*R*) diastereomer of acoltremon, C₁₈H₂₇NO₂, from synchrotron powder diffraction data and density functional theory calculations

Jacob K. Salazar, James A. Kaduk, Anja Dosen and Thomas N. Blanton

Computing details

(1*R*,2*S*,5*R*)-2-Isopropyl-*N*-(4-methoxyphenyl)-5-methylcyclohexane-1-carboxamide (acoltremon_2)

Crystal data

C ₁₈ H ₂₇ NO ₂	$V = 1726.59 (1) \text{ \AA}^3$
$M_r = 289.42$	$Z = 4$
Orthorhombic, $P2_12_12_1$	$D_x = 1.113 \text{ Mg m}^{-3}$
$a = 9.320220 (15) \text{ \AA}$	Synchrotron radiation, $\lambda = 0.46873 \text{ \AA}$
$b = 11.39111 (3) \text{ \AA}$	$T = 295 \text{ K}$
$c = 16.26284 (4) \text{ \AA}$	cylinder, $2.0 \times 1.5 \text{ mm}$

Data collection

11-BM, APS diffractometer	Data collection mode: transmission
Specimen mounting: Kapton capillary	Scan method: step
	$2\theta_{\min} = 0.510^\circ$, $2\theta_{\max} = 49.995^\circ$, $2\theta_{\text{step}} = 0.001^\circ$

Refinement

Least-squares matrix: full	53 restraints
$R_p = 0.113$	16 constraints
$R_{\text{wp}} = 0.133$	Weighting scheme based on measured s.u.'s
$R_{\text{exp}} = 0.038$	$(\Delta/\sigma)_{\max} = 1.712$
$R(F^2) = 0.10052$	Background function: Background function:
49486 data points	"chebyshev-1" function with 6 terms:
Profile function: Finger-Cox-Jephcoat function	47.29(16), -6.65(24), -12.59(16), 2.79(16),
parameters U, V, W, X, Y, SH/L: peak	-3.99(17), -0.00(16), Background peak
variance(Gauss) = $U \tan(\text{Th})^2 + V \tan(\text{Th}) + W$:	parameters: pos, int, sig, gam: 6.167(16),
peak HW(Lorentz) = $X/\cos(\text{Th}) + Y \tan(\text{Th})$;	1.122(32)e4, 1.24(5)e4, 0.100,
SH/L = S/L + H/L U, V, W in (centideg) ² , X & Y	Preferred orientation correction: Simple
in centideg 2.543, -0.174, 0.052, 0.000, 0.000,	spherical harmonic correction Order = 2
0.002,	Coefficients: 0:0:C(2,0) = 0.290(5); 0:0:C(2,2)
83 parameters	= 0.295(3)

Fractional atomic coordinates and isotropic or equivalent isotropic displacement parameters (\AA^2)

	<i>x</i>	<i>y</i>	<i>z</i>	$U_{\text{iso}}^*/U_{\text{eq}}$
O1	1.0060 (5)	0.3097 (4)	0.5123 (3)	0.0774 (13)*
O2	0.9044 (5)	0.1119 (5)	0.8745 (3)	0.122 (2)*

N3	0.7965 (5)	0.2314 (5)	0.5481 (3)	0.0774 (13)*
C4	0.8275 (6)	0.4484 (4)	0.4087 (3)	0.0785 (11)*
C5	0.8154 (5)	0.3208 (4)	0.4181 (3)	0.0785 (11)*
C6	0.7586 (6)	0.4837 (5)	0.3279 (4)	0.0785 (11)*
C7	0.8365 (6)	0.2953 (5)	0.2633 (3)	0.0785 (11)*
C8	0.8992 (6)	0.2713 (5)	0.3472 (4)	0.0785 (11)*
C9	0.8316 (7)	0.4299 (6)	0.2550 (3)	0.0785 (11)*
C10	0.7665 (7)	0.5165 (6)	0.4855 (4)	0.124 (2)*
C11	0.8833 (5)	0.2836 (5)	0.4956 (3)	0.0774 (13)*
C12	0.9335 (7)	0.2360 (6)	0.1913 (3)	0.0785 (11)*
C13	0.7878 (7)	0.6442 (7)	0.4737 (4)	0.124 (2)*
C14	0.5992 (7)	0.5117 (7)	0.4841 (5)	0.124 (2)*
C15	0.8281 (7)	0.2023 (6)	0.6291 (3)	0.0637 (11)*
C16	0.7831 (7)	0.0934 (5)	0.6598 (3)	0.0637 (11)*
C17	0.8947 (7)	0.2790 (4)	0.6808 (4)	0.0637 (11)*
C18	0.8106 (7)	0.0608 (5)	0.7419 (4)	0.0637 (11)*
C19	0.9405 (6)	0.2401 (5)	0.7600 (4)	0.0637 (11)*
C20	0.8859 (7)	0.1368 (6)	0.7939 (3)	0.0637 (11)*
C21	0.8311 (7)	0.0201 (7)	0.9119 (4)	0.122 (2)*
H22	0.94662	0.47012	0.40403	0.0942*
H23	0.69849	0.29161	0.41551	0.0942*
H24	0.76261	0.58335	0.32187	0.0942*
H25	0.64173	0.45417	0.32732	0.0942*
H26	0.72280	0.25865	0.26023	0.0942*
H27	1.01186	0.31027	0.34713	0.0942*
H28	0.90827	0.17223	0.35567	0.0942*
H29	0.77023	0.45365	0.19669	0.0942*
H30	0.94572	0.46530	0.25046	0.0942*
H31	0.81334	0.48356	0.54600	0.1482*
H32	1.05097	0.26012	0.20108	0.0942*
H33	0.92100	0.13649	0.19352	0.0942*
H34	0.89651	0.26980	0.12882	0.0942*
H35	0.68069	0.69145	0.48081	0.1482*
H36	0.83250	0.66107	0.40953	0.1482*
H37	0.86659	0.67839	0.52166	0.1482*
H38	0.56192	0.41944	0.50089	0.1482*
H39	0.55441	0.57720	0.53046	0.1482*
H40	0.55903	0.53493	0.41992	0.1482*
H41	0.69380	0.20820	0.53000	0.0928*
H42	0.72320	0.02953	0.61815	0.0764*
H43	0.91356	0.37362	0.66070	0.0764*
H44	0.77148	-0.02757	0.76598	0.0764*
H45	1.02243	0.29354	0.79616	0.0764*
H46	0.91141	-0.04652	0.93674	0.1460*
H47	0.75825	-0.02427	0.86494	0.1460*
H48	0.76348	0.05576	0.96470	0.1460*

Geometric parameters (Å, °)

O1—C11	1.213 (4)	C15—N3	1.391 (4)
O2—C20	1.352 (5)	C15—C16	1.402 (5)
O2—C21	1.389 (7)	C15—C17	1.362 (4)
N3—C11	1.317 (5)	C16—C15	1.402 (5)
N3—C15	1.391 (4)	C16—C18	1.410 (4)
N3—H41	1.035 (4)	C16—H42	1.140 (4)
C4—C5	1.465 (5)	C17—C15	1.362 (4)
C4—C6	1.517 (5)	C17—C19	1.428 (5)
C4—C10	1.575 (5)	C17—H43	1.139 (4)
C4—H22	1.140 (5)	C18—C16	1.410 (4)
C5—C4	1.465 (5)	C18—C20	1.399 (5)
C5—C8	1.502 (4)	C18—H44	1.140 (4)
C5—C11	1.472 (4)	C19—C17	1.428 (5)
C5—H23	1.140 (5)	C19—C20	1.395 (5)
C6—C4	1.517 (5)	C19—H45	1.140 (4)
C6—C9	1.498 (5)	C20—O2	1.352 (5)
C6—H24	1.141 (6)	C20—C18	1.399 (5)
C6—H25	1.140 (6)	C20—C19	1.395 (5)
C7—C8	1.509 (6)	C21—O2	1.389 (7)
C7—C9	1.540 (6)	C21—H46	1.139 (8)
C7—C12	1.626 (6)	C21—H47	1.140 (7)
C7—H26	1.140 (6)	C21—H48	1.140 (7)
C8—C5	1.502 (4)	H22—C4	1.140 (5)
C8—C7	1.509 (6)	H23—C5	1.140 (5)
C8—H27	1.140 (6)	H24—C6	1.141 (6)
C8—H28	1.140 (6)	H25—C6	1.140 (6)
C9—C6	1.498 (5)	H26—C7	1.140 (6)
C9—C7	1.540 (6)	H27—C8	1.140 (6)
C9—H29	1.140 (5)	H28—C8	1.140 (6)
C9—H30	1.140 (6)	H29—C9	1.140 (5)
C10—C4	1.575 (5)	H30—C9	1.140 (6)
C10—C13	1.481 (8)	H31—C10	1.140 (6)
C10—C14	1.561 (6)	H32—C12	1.140 (7)
C10—H31	1.140 (6)	H33—C12	1.140 (7)
C11—O1	1.213 (4)	H34—C12	1.140 (6)
C11—N3	1.317 (5)	H35—C13	1.140 (7)
C11—C5	1.472 (4)	H36—C13	1.140 (7)
C12—C7	1.626 (6)	H37—C13	1.140 (7)
C12—H32	1.140 (7)	H38—C14	1.140 (7)
C12—H33	1.140 (7)	H39—C14	1.140 (7)
C12—H34	1.140 (6)	H40—C14	1.140 (7)
C13—C10	1.481 (8)	H41—N3	1.035 (4)
C13—H35	1.140 (7)	H42—C16	1.140 (4)
C13—H36	1.140 (7)	H43—C17	1.139 (4)
C13—H37	1.140 (7)	H44—C18	1.140 (4)
C14—C10	1.561 (6)	H45—C19	1.140 (4)

C14—H38	1.140 (7)	H46—C21	1.139 (8)
C14—H39	1.140 (7)	H47—C21	1.140 (7)
C14—H40	1.140 (7)	H48—C21	1.140 (7)
C20—O2—C21	121.3 (5)	H32—C12—H33	109.5 (5)
C11—N3—C15	126.2 (4)	H32—C12—H34	109.5 (5)
C11—N3—H41	119.9 (4)	H33—C12—H34	109.4 (5)
C15—N3—H41	113.8 (5)	C10—C13—H35	109.4 (6)
C5—C4—C6	108.7 (4)	C10—C13—H36	109.4 (6)
C5—C4—H22	107.3 (4)	H35—C13—H36	109.5 (6)
C6—C4—H22	107.3 (5)	C10—C13—H37	109.5 (7)
C4—C5—C8	104.6 (4)	H35—C13—H37	109.5 (6)
C4—C5—C11	110.0 (3)	H36—C13—H37	109.5 (5)
C8—C5—C11	109.0 (4)	C10—C14—H38	109.4 (6)
C4—C5—H23	111.1 (4)	C10—C14—H39	109.5 (6)
C8—C5—H23	111.0 (4)	H38—C14—H39	109.5 (6)
C11—C5—H23	111.0 (4)	C10—C14—H40	109.4 (5)
C4—C6—C9	112.7 (4)	H38—C14—H40	109.5 (6)
C4—C6—H24	108.9 (5)	H39—C14—H40	109.5 (6)
C9—C6—H24	108.9 (5)	N3—C15—C16	119.0 (5)
C4—C6—H25	109.5 (5)	N3—C15—C17	121.9 (5)
C9—C6—H25	107.9 (5)	C16—C15—C17	119.0 (3)
H24—C6—H25	108.9 (4)	C15—C16—C18	121.0 (3)
C8—C7—C9	105.7 (4)	C15—C16—H42	120.0 (5)
C8—C7—H26	109.5 (5)	C18—C16—H42	119.0 (5)
C9—C7—H26	109.4 (5)	C15—C17—C19	119.6 (3)
C5—C8—C7	115.1 (4)	C15—C17—H43	120.0 (5)
C5—C8—H27	109.5 (5)	C19—C17—H43	120.4 (5)
C7—C8—H27	106.5 (5)	C16—C18—C20	120.1 (3)
C5—C8—H28	108.5 (5)	C16—C18—H44	119.9 (5)
C7—C8—H28	108.4 (5)	C20—C18—H44	120.0 (5)
H27—C8—H28	108.5 (4)	C17—C19—C20	120.6 (3)
C6—C9—C7	110.5 (4)	C17—C19—H45	120.0 (6)
C6—C9—H29	109.5 (5)	C20—C19—H45	119.4 (6)
C7—C9—H29	108.9 (5)	O2—C20—C18	121.3 (5)
C6—C9—H30	109.3 (6)	O2—C20—C19	120.9 (5)
C7—C9—H30	109.3 (5)	C18—C20—C19	117.8 (3)
H29—C9—H30	109.3 (4)	O2—C21—H46	109.5 (6)
C13—C10—C14	99.6 (5)	O2—C21—H47	109.4 (5)
C13—C10—H31	112.5 (6)	H46—C21—H47	109.5 (7)
C14—C10—H31	112.5 (6)	O2—C21—H48	109.4 (7)
O1—C11—N3	123.0 (4)	H46—C21—H48	109.5 (5)
O1—C11—C5	121.7 (3)	H47—C21—H48	109.5 (6)
N3—C11—C5	114.9 (3)		

(acoltremon_2_VASP)

Crystal data $C_{18}H_{27}NO_2$ $M_r = 289.42$ Orthorhombic, $P2_12_12_1$ $a = 9.32022 \text{ \AA}$ $b = 11.39111 \text{ \AA}$ $c = 16.26284 \text{ \AA}$ $V = 1726.59 \text{ \AA}^3$ $Z = 4$ *Data collection* $h = \rightarrow$ $l = \rightarrow$ $k = \rightarrow$ *Fractional atomic coordinates and isotropic or equivalent isotropic displacement parameters (\AA^2)*

	<i>x</i>	<i>y</i>	<i>z</i>	$B_{\text{iso}}^*/B_{\text{eq}}$
O1	1.01413	0.30651	0.51100	
O2	0.90354	0.11941	0.87778	
N3	0.79574	0.23233	0.54912	
C4	0.82622	0.46054	0.40507	
C5	0.81815	0.32519	0.41433	
C6	0.76351	0.49545	0.32138	
C7	0.84080	0.30145	0.25810	
C8	0.89693	0.26450	0.34276	
C9	0.84152	0.43556	0.25010	
C10	0.76145	0.52847	0.47885	
C11	0.88472	0.28716	0.49524	
C12	0.92763	0.24298	0.18986	
C13	0.80650	0.65778	0.47776	
C14	0.59804	0.51763	0.48653	
C15	0.83074	0.19945	0.63072	
C16	0.77289	0.09627	0.66346	
C17	0.91421	0.27182	0.68170	
C18	0.79465	0.06595	0.74578	
C19	0.93765	0.24165	0.76324	
C20	0.87726	0.13914	0.79624	
C21	0.81861	0.03231	0.91816	
H22	0.94183	0.48270	0.40418	
H23	0.70449	0.29852	0.41349	
H24	0.76879	0.59126	0.31368	
H25	0.64871	0.47176	0.31927	
H26	0.72797	0.27240	0.25317	
H27	1.01212	0.28588	0.34672	
H28	0.88899	0.16829	0.34954	
H29	0.79251	0.46137	0.19103	
H30	0.95403	0.46632	0.24810	
H31	0.80890	0.48978	0.53495	
H32	1.04086	0.27042	0.19257	
H33	0.92576	0.14661	0.19508	
H34	0.88640	0.26639	0.12866	

H35	0.75606	0.70558	0.42664
H36	0.92354	0.66743	0.47264
H37	0.77364	0.70176	0.53494
H38	0.56228	0.42571	0.48786
H39	0.56132	0.55978	0.54368
H40	0.54279	0.56176	0.43530
H41	0.69185	0.21534	0.52992
H42	0.70813	0.03924	0.62428
H43	0.95775	0.35348	0.65753
H44	0.74655	-0.01411	0.76994
H45	0.99958	0.29888	0.80367
H46	0.84877	0.03673	0.98317
H47	0.84234	-0.05661	0.89556
H48	0.70326	0.05132	0.91125

Hydrogen-bond geometry (Å, °)

<i>D</i> —H \cdots <i>A</i>	<i>D</i> —H	H \cdots <i>A</i>	<i>D</i> \cdots <i>A</i>	<i>D</i> —H \cdots <i>A</i>
N3—H41 \cdots O1 ⁱ	1.04	1.80	2.836	175
C5—H23 \cdots O1 ⁱ	1.10	2.47	3.428	145
C13—H35 \cdots O2	1.10	2.61	3.594	148
C10—H31 \cdots C11 ⁱⁱ	1.11	2.50	2.991	106

Symmetry codes: (i) $-x-1, y+1/2, -z+3/2$; (ii) $x+5/2, -y-1/2, -z+1$.**(Molecules_100K_VASP)***Crystal data* $C_{18}H_{27}NO_2$ $M_r = 289.42$ $P2_12_12_1$ $a = 9.13710 \text{ \AA}$ $b = 10.38210 \text{ \AA}$ $c = 17.48930 \text{ \AA}$ $\alpha = 90^\circ$ $\beta = 90^\circ$ $\gamma = 90^\circ$ $V = 1659.07 \text{ \AA}^3$ $Z = 4$ *Data collection* $h = \rightarrow$ $k = \rightarrow$ $l = \rightarrow$ *Fractional atomic coordinates and isotropic or equivalent isotropic displacement parameters (Å²)*

	<i>x</i>	<i>y</i>	<i>z</i>	U_{iso}^*/U_{eq}
O1	0.8885	0.6624	0.5105	?
O2	0.9034	0.0242	0.8026	?
N1	0.6836	0.7769	0.5428	?
C1	0.4621	0.4887	0.5510	?
C2	0.6165	0.2918	0.5384	?
C3	0.6132	0.4381	0.5276	?
C4	0.6568	0.4789	0.4455	?
C5	0.7971	0.4126	0.4174	?
C6	0.8423	0.4550	0.3372	?

C7	0.8627	0.6007	0.3317	?
C8	0.9099	0.6428	0.2520	?
C9	0.7217	0.6676	0.3564	?
C10	0.6655	0.6279	0.4362	?
C11	0.7566	0.6895	0.4990	?
C12	0.7420	0.8372	0.6090	?
C13	0.8065	0.7644	0.6670	?
C14	0.8608	0.8232	0.7329	?
C15	0.8508	0.9571	0.7411	?
C16	0.7842	0.0306	0.6835	?
C17	0.7303	0.9709	0.6182	?
C18	0.9601	0.9513	0.8652	?
H1N	0.5786	0.8009	0.5264	?
H1A	0.4530	0.5939	0.5468	?
H1B	0.4372	0.4617	0.6104	?
H1C	0.3768	0.4467	0.5142	?
H2A	0.5461	0.2438	0.4959	?
H2B	0.5744	0.2658	0.5953	?
H2C	0.7273	0.2517	0.5331	?
H00F	0.6953	0.4796	0.5671	?
H4	0.5669	0.4483	0.4070	?
H5A	0.8866	0.4336	0.4578	?
H5B	0.7817	0.3074	0.4178	?
H6A	0.9438	0.4055	0.3201	?
H6B	0.7577	0.4254	0.2955	?
H7	0.9499	0.6281	0.3720	?
H8A	0.8272	0.6157	0.2090	?
H8B	0.0141	0.5972	0.2357	?
H8C	0.9255	0.7478	0.2491	?
H9A	0.6348	0.6435	0.3149	?
H9B	0.7337	0.7731	0.3539	?
H10	0.5539	0.6665	0.4413	?
H13	0.8143	0.6603	0.6610	?
H14	0.9108	0.7635	0.7769	?
H16	0.7757	0.1346	0.6910	?
H17	0.6780	0.0285	0.5738	?
H18A	0.8752	0.8875	0.8892	?
H18B	0.9948	0.0218	0.9082	?
H18C	0.0551	0.8926	0.8477	?

Hydrogen-bond geometry (Å, °)

<i>D—H···A</i>	<i>D—H</i>	<i>H···A</i>	<i>D···A</i>	<i>D—H···A</i>
N1—H1N···O1	1.03	1.89	2.922	176
C18—H18B···O1	1.10	2.30	3.383	169
C10—H10···O1	1.10	2.48	3.466	149
C9—H9B···O2	1.10	2.61	3.526	140
C3—H00F···C11	1.11	2.55	2.963	101
